

Conodont Biostratigraphic Constraint on the Lower Taiyuan Formation in Southern North China and Its Paleogeographic Implications



Yuan Wang¹, Jianghai Yang^{*1,2}, Dong-Xun Yuan^{3,4}, Jia Liu¹, Rui Ma¹

1. School of Earth Sciences, China University of Geosciences, Wuhan 430074, China

2. State Key Laboratory of Biogeology and Environmental Geology, China University of Geosciences, Wuhan 430074, China

3. School of Resources and Geosciences, China University of Mining and Technology, Xuzhou 221116, China

4. State Key Laboratory of Palaeobiology and Stratigraphy, Nanjing Institute of Geology and Palaeontology and Center for Excellence in Life and Palaeoenvironment, Chinese Academy of Sciences, Nanjing 210008, China

 Yuan Wang: <https://orcid.org/0000-0002-9932-0973>;  Jianghai Yang: <https://orcid.org/0000-0002-5238-8655>

ABSTRACT: The Late Paleozoic Taiyuan Formation in North China is mainly composed of a mixed shallow-marine carbonate and terrigenous clastic deposits. Its basal limestones have been constrained in the late Pennsylvanian to Early Permian. To further constrain the age of the lowest Taiyuan Formation, we obtained two genera and 16 species of conodonts from the bottom limestones of the Taiyuan Formation in two sections in Henan Province, southern North China. The fauna includes *Idiognathodus hebeiensis*, *Streptognathodus isolatus*, *S. elongatus*, *S. cf. longus*, *S. acuminatus*, *S. cf. recreatus*, *S. cf. cristellaris*, *S. bellus*, *S. invaginatus*, *S. wabaunsensis*, *S. glenisteri*, *S. conjunctus*, *S. binodosus*, *S. fuchengensis*, *S. nodularis*, and *S. sp.* A genus of *Streptognathodus* dominated conodont assemblage with some *Idiognathodus* elements. It indicates a late Gzhelian (latest Pennsylvanian) age for the lowest Taiyuan Formation in southern North China. This is consistent with recently published high-precision zircon U-Pb ages from ash layers. Based on conodont biostratigraphy, the basal limestones of the Taiyuan Formation in Henan Province (southern North China) can be correlated with the upper part of Miaogou limestones of the Taiyuan Formation in Shanxi Province (northern North China). This correlation might reflect a significant sea-level rise in North China, possibly corresponding to a deglaciation event at the Permo-Carboniferous transition.

KEY WORDS: Taiyuan Formation, conodonts, Gzhelian, southern North China, biostratigraphy.

0 INTRODUCTION

The Late Paleozoic witnessed the longest-lived glaciation in the Phanerozoic and was associated with variations in atmospheric $p\text{CO}_2$ and glacial-eustasy (Montañez et al., 2016, 2007; Saltzman, 2003). The acme of Late Paleozoic Ice Age (LPIA) has been constrained in the Latest Carboniferous to Early Permian (Soreghan et al., 2019; Montañez and Poulsen, 2013; Isbell et al., 2003; Frakes et al., 1992; Veevers and Powell, 1987). During the Permo-Carboniferous glaciation, cyclothemic depositions of limestones and shales were formed in the Midcontinent of North America along the western tropical Pangea and have been linked to the glacial relative sea-level changes (Heckel, 2008, 1994; Joeckel, 1999, 1994). Conodont-based biostratigraphic correlations of the cyclothems have been recognized in U.S. Midcontinent, Russian Platform or East-Europe Platform,

corresponding to the glacial-deglacial cycles of Gondwana ice sheets (Heckel, 2008; Heckel et al., 2007, 2005). Similar cyclothemic successions have also developed in the Taiyuan Formation in North China (Wang, 2010; Shang, 1997; Li et al., 1996; Fan, 1991). The Taiyuan Formation was a mixed sequence of shallow marine carbonates and terrigenous clastic rocks. However, correlation between Taiyuan Formation and sedimentary records in North America and its global implications are largely impeded by the poor age constraint.

Conodonts are important index fossils for providing a time scale based on the changes or evolution of shape and widespread distribution (e.g., Shen et al., 2019; Henderson, 2018). A large number of studies on Permian to Triassic conodont biostratigraphy have been concluded (Wu B J et al., 2021; Zakharov et al., 2021; Liu et al., 2020), however, in North China, only a few studies on Late Paleozoic conodont assemblages have been published (e.g., Gao et al., 2005; Wang and Qi, 2003; Wan et al., 1983), and the precise age is still highly debated for the lower Taiyuan Formation of Henan Province (Pei, 2004; Wang and Qi, 2003). The Taiyuan Formation has been biostratigraphically thought to be of Early Permian age (Song et al., 2014; Wang and Qi, 2003) or considered to partially extend

*Corresponding author: yangjh@cug.edu.cn

© China University of Geosciences (Wuhan) and Springer-Verlag GmbH Germany, Part of Springer Nature 2022

Manuscript received May 18, 2021.

Manuscript accepted July 29, 2021.

to Late Carboniferous in age (Li et al., 2013; Wang, 2010). Such disputations on the age of Taiyuan Formation led to controversial stratigraphic correlations of Permo-Carboniferous strata across North China (Pei, 1999; Zhang et al., 1988; Wan et al., 1983). Newly reported high-precision zircon U-Pb ages tend to constrain the lower Taiyuan Formation in the Latest Carboniferous (Wu Q et al., 2021; Yang J H et al., 2020). To examine this radio-isotopic ages and further constrain the age of Taiyuan Formation, in this study, we focus on the conodont biostratigraphy of the basal Taiyuan Formation in southern North China and its further correlation with the counterparts in northern North China.

1 GEOLOGICAL SETTING AND SAMPLED SUCCESIONS

The North China Craton is surrounded by the Central Asia Orogen to the north, the Qilian Orogen to the west and the Qinling-Dabie-Sulu Orogen to the south and east (Fig. 1a; Yang Z L et al., 2021; Yang C H et al., 2020; Zhai and Santosh, 2013, 2011; Li et al., 2010; Zhao et al., 2005), which is the largest and oldest craton in eastern Eurasia. Metamorphic basement of the Early Precambrian is widely exposed (Huang et al., 2020; Wan et al., 2020), on which there is a set of Cambrian-Ordovician carbonates. A widespread unconformity developed between the underlying Cambrian-Ordovician sediments and the overlying Carboniferous-Permian carbonate and siliciclastic successions (Tang, 1989; Wang and Li, 1984). The Permo-Carboniferous strata in North China generally include, in ascending order, the Benxi, Taiyuan, Shanxi, Xiashihezi, Shangshihezi and Shiqianfeng formations. The Taiyuan Formation was originally defined as a set of coal-bearing successions of marine carbonate and clastic rocks in Shanxi Province (Weng and Grabau, 1925). This stratigraphic unit currently refers to multiple cyclic layers of limestones, mudrocks and sandstones with intercalated coals. It overlies the bauxitic mudrocks of the Benxi Formation and underlies the sandstones and mudrocks

of the Shanxi Formation (Pei, 1999). In the stratotype section in Xishan region of Shanxi Province, there developed five major limestone beds in the Taiyuan Formation, named Wujiayu, Miaogou, Maogou, Xiedao and Dongdayao limestones in ascending order (Pei, 1999; Wang et al., 1990). In northern North China, these five limestone beds can be tracked widely in Shanxi, Hebei and Shandong provinces, and represent significant marine transgression events (Lü et al., 2009; Fan, 1991; Zhang, 1989). They yielded conodonts and fusulinids and were constrained in the Late Carboniferous to Early Permian (Song et al., 2014; Su et al., 2006; Gao et al., 2005; Pei, 2004; Wang and Qi, 2003; Jiang et al., 2002; Wang, 1991; Liang, 1989; Zhang et al., 1988; Xia et al., 1987; Wan and Ding, 1984; Wan et al., 1983).

In Henan Province of southern North China, the Permo-Carboniferous strata mainly outcropped in its northwestern and central parts (Fig. 1b) and have also been revealed in drilling cores in eastern and southern parts (e.g., Yang J H et al., 2020; Song et al., 2011). In the studied area, the Taiyuan Formation was usually 10 to 60 m thick and characterized by four bioclastic limestones with intercalated thin-bedded marls and mudrocks in the lower part, thin- to medium-bedded quartzose sandstones and mudrocks in the middle part and thick-bedded cherty limestones in the upper part. Marine limestones of the Taiyuan Formation have been studied for biostratigraphy (Li et al., 2013; Pei, 1999; Liang, 1994; Zhao and Liang, 1994; Lin and Mao, 1990; Zhang, 1989; Zhang et al., 1988; Wan and Ding, 1987; Zheng, 1987), but with low sampling resolution. For this study, the lowest Taiyuan Formation of Wenwan and Baipohe sections were sampled for high-resolution conodont biostratigraphy (Fig. 1b). The Wenwan Section is located ~34 km to the west of Yuzhou City and close (~4 km) to the Dafengkou Section (Zhang et al., 1988; Wan and Ding, 1987). There the Taiyuan Formation is conformably overlying the bauxitic mudrocks with siderite oolites of the Benxi Formation and its lower part consists of limestones with intercalated coals

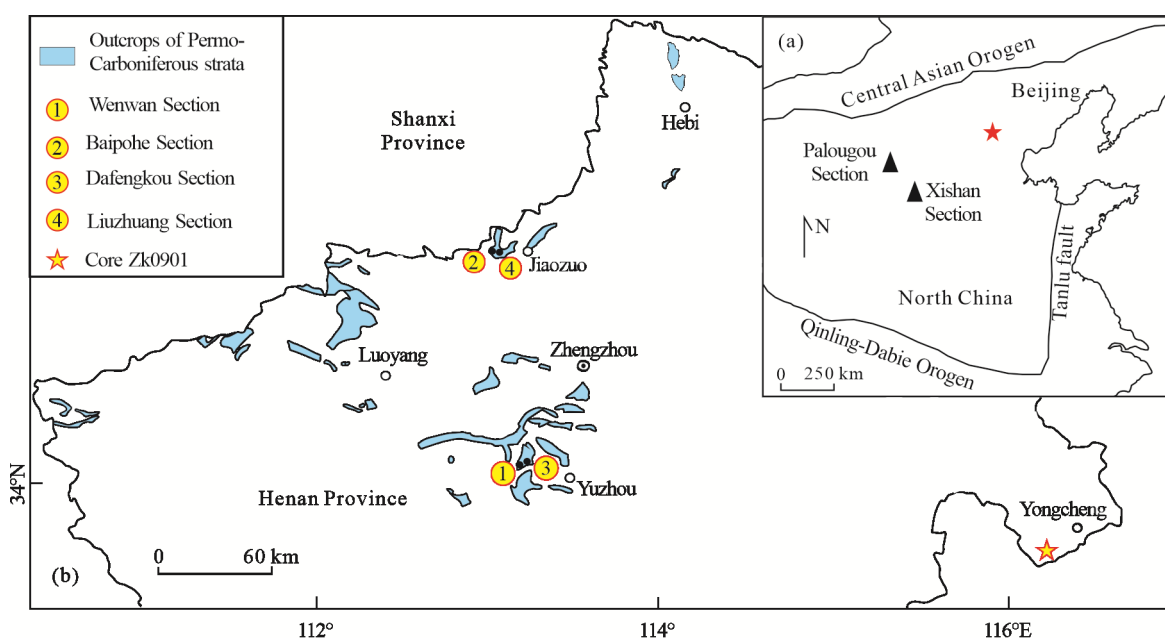


Figure 1. Sketch maps showing the paleogeographic units of the North China (a) and the Permo-Carboniferous outcrops in Henan Province (b).

and mudrocks. The Baipohe Section is located about 20 km to the northwest of Jiaozuo and close (~2.5 km) to the Liuzhuang Section (Lin and Mao, 1990). There outcropped the lower Taiyuan Formation conformably overlying the bauxitic mudrocks of the Benxi Formation and consisting of limestones and mudstones (Fig. 2).

2 RESULTS

Conodonts were collected from the bottom limestones of the Taiyuan Formation in the Wenwan and Baipohe sections. In the Wenwan Section, two genera and 13 species were recognized, including *Streptognathodus elongatus* Gunnell, 1933, *S. wabaunsensis* Gunnell, 1933, *S. acuminatus* Gunnell, Chernykh & Reshetkova, 1987, *S. bellus* Chernykh & Ritter, 1997, *S. cf. longus* Chernykh, 2005, *S. cf. cristellaris* Chernykh & Reshetkova, 1987, *S. cf. recreatus* Chernykh, 2005, *S. invaginatus* Reshetkova & Chernykh, 1986, *S. isolatus* Chernykh, Ritter & Wardlaw, 1997, *S. fuchengensis* Zhao, 1981, *S. binodosus* Wardlaw, Boardman & Nestell, 2009, *Streptognathodus* sp. and *Idiognathodus hebeiensis* Zhao & Wan, 1981. A comparable conodont fauna, including *Idiognathodus hebeiensis*, *I. tersus*, *Streptognathodus elongatus*, *S. graclis*, *S. oppletus*, *S. elegantulus* and *S. wabaunsensis*, was discovered from the bottom limestones of the Taiyuan Formation in the nearby Dafengkou Section (Zhang et al., 1988). In the Baipohe Section, two genera and 13 species were recognized, most conodonts of the section belong to *Streptognathodus* (Fig. 2). They are *Idiognathodus hebeiensis* Zhao & Wan, 1984, *Streptognathodus elongatus*

Gunnell, 1933, *S. bellus* Chernykh & Ritter, 1997, *S. acuminatus* Gunnell, Chernykh & Reshetkova, 1987, *S. wabaunsensis* Gunnell, 1933, *S. conjunctus* Barskov, Isakova & Shchastlivceva, 1981, *S. binodosus* Wardlaw, Boardman & Nestell, 2009, *S. isolatus* Chernykh, Ritter & Wardlaw, 1997, *S. nodulinearis* Reshetkova & Chernykh, 1986, *S. glenisteri* Chernykh & Ritter, 1997, *S. cf. recreatus* Chernykh, 2005, *S. fuchengensis* Zhao, 1981 and *Streptognathodus* sp. The asymmetrical *Idiognathodus* represent a distinct clade of species with strong dextral-sinistral Pa element asymmetry during the late Pennsylvanian (Hogancamp, 2020). The features possessed by species are ensured through robust platform, continuous transverse ridges, well-developed inner lobes, and less apparent eccentric groove. Based on these characteristics, the species are identified as *Idiognathodus hebeiensis* in Taiyuan Formation (Zhao and Wan, 1983). A similar conodont fauna, including *I. tersus*, *S. elongatus*, *S. graclis*, *S. parvus*, *S. oppletus* were also obtained from the bottom limestones of the Taiyuan Formation in the nearby Liuzhuang Section (Lin and Mao, 1990).

The *Streptognathodus* species are commonly found in the lower Taiyuan Formation. According to the lineages of *Streptognathodus* species proposed by Boardman et al. (2009) and Chernykh (2020, 2010), *S. bellus* probably is the root stock for most of the *Streptognathodus* species around the Carboniferous-Permian boundary, which evolved to elongate, robust and nodular forms based on this species (Boardman et al., 2009). The species of *S. elongatus* and *S. cf. longus* have a typical elongate platform in both late Gzhelian and early Asselian

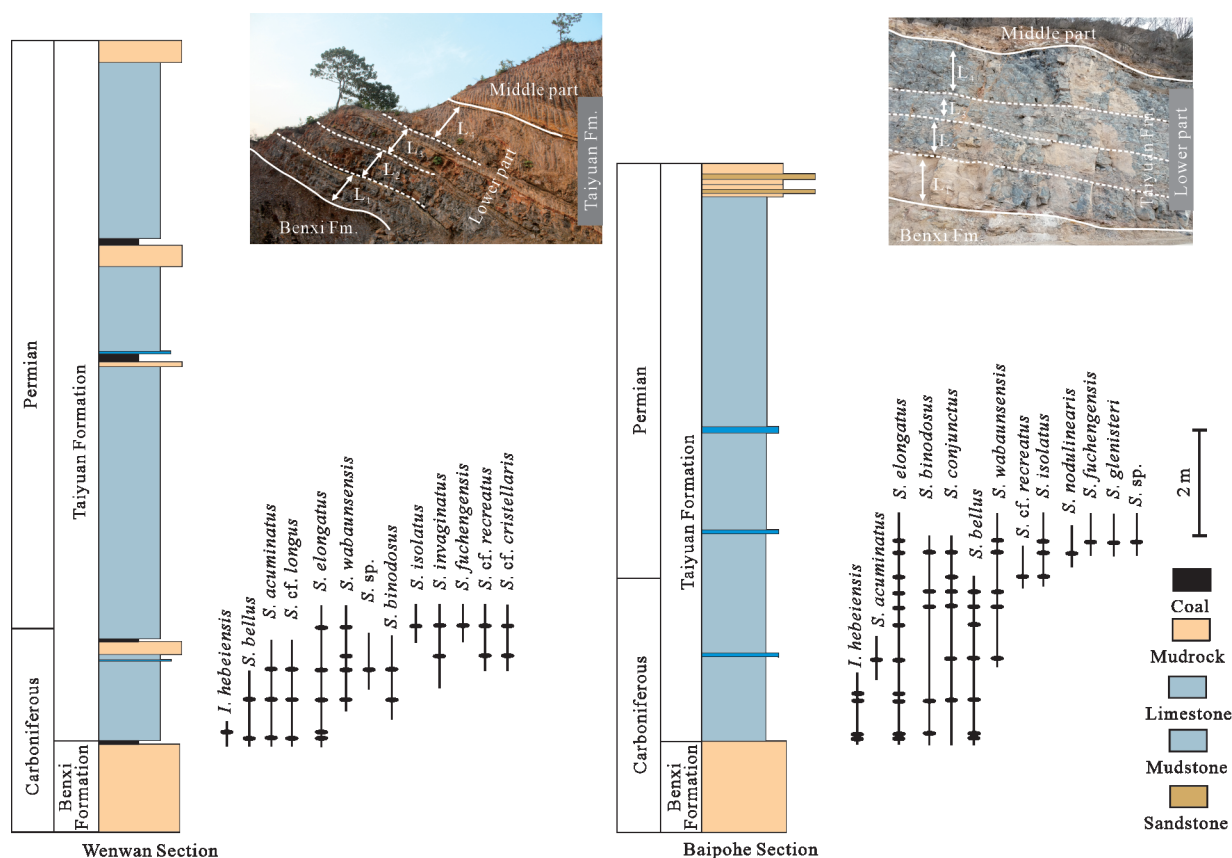


Figure 2. Stratigraphical column and field photographs showing the established conodont biostratigraphy of the lower Taiyuan Formation in the Wenwan and Baipohe sections.

(Chernykh, 2020, 2010; Boardman et al., 2009; Stauffer and Plummer, 1932). The morphological evolution of *Streptognathodus* in the latest Gzhelian and early Asselian showed trends from *S. bellus*-*S. wabaunsensis*-*S. isolatus*-*S. glenisteri*-*S. cristellaris*-*S. recreatus* lineage (Chernykh, 2010). The *S. wabaunsensis* has typical features of irregularly arranged nodes on the oral surface, and the node field is not separated from the carina. In the basal part of the Taiyuan Formation, conodont samples with apparent nodes are in parapet and shallow median groove were identified as juvenile *S. wabaunsensis* (Chernykh and Ritter, 1997; Gunnell, 1933). Those linear arrangements of accessory nodes were identified as *S. nodulinearis* (Reshetkova and Chernykh, 1986). Boardman et al. (2009) considered that *S. nodulinearis* are descendants of *S. wabaunsensis* in the upper Hughes Creek Shale Member and may also occur in the Urals of Russia. The species of *S. isolatus* mark the lower boundary of Asselian and are characterized by inner accessory lobe separated from the carina by a moat-like trough (Chernykh et al., 1997). *Streptognathodus invaginatus* has a typical character which is a distinct inflection on the inner parapet with one to three accessory denticles (Boardman et al., 2009; Reshetkova and Chernykh, 1986). Other conodonts, like *S. fuchengensis*, *S. glenisteri*, *S. cf. cristellaris*, *S. cf. recreatus*, are emerged early in the Asselian (Chernykh, 2020, 2006, 2005; Boardman et al., 2009).

3 DISCUSSION

3.1 Age of the Lower Taiyuan Formation in Henan Province

In Henan Province, the bottom limestones of the Taiyuan Formation contain a conodont fauna dominated by *Idiognathodus* and *Streptognathodus* (Fig. 2). The asymmetrical *Idiognathodus* represent a distinct clade of species, which had a wide geographic distribution in the late Pennsylvanian (Wang et al., 2019; Sobolev and Nakrem, 1996; Chernikh and Reshetkova, 1987). Of the identified *Idiognathodus* elements, *I. hebeiensis* is unique and has also been reported from the bottom limestone of Taiyuan Formation in North China and Shazitang Formation in South China (Zhao, 1989; Zhao and Wan, 1983). Of the identified *Streptognathodus* elements, *Streptognathodus bellus* appeared in latest Gzhelian and extended to earliest Asselian in Moscow Basin, South Urals, U.S. Midcontinent and South China (Chernykh, 2020, 2002; Hu et al., 2020; Barrick et al., 2013; Boardman et al., 2009; Alekseev and Goreva, 2007). *S. bellus*, *S. elongatus*, *S. conjunctus*, *S. acminacutus*, *S. cf. longus*, *S. binodosus*, *S. nodulinearis* and *S. wabaunsensis* generally also have an extending age distribution from the late Pennsylvanian to early Asselian. *Streptognathodus fuchengensis*, *S. cf. recreatus*, *S. invaginatus*, *S. cf. cristellaris*, *S. glenisteri* were shown in early Asselian strata of North America and Russia Platform (Chernykh, 2010, 2006, 2005; Boardman et al., 2009). In contrast, *S. wabaunsensis* has a more distinct stratigraphic significance and its first appearance marks the *S. wabaunsensis* Zone, the highest Pennsylvanian conodont zone, in South China, Russia and Ural (Hu et al., 2020; Wang et al., 2019; Henderson, 2018; Goreva and Alekseev, 2010; Wang and Qi, 2003). Another species with stratigraphic significance is *Streptognathodus isolatus*, which developed from an advanced morphotype in the *S. wabaunsensis* chronocline and whose first appearance

marks the Permo-Carboniferous boundary (Chernykh and Ritter, 1997). For the two studied sections, *S. wabaunsensis* has a local first occurrence in the bottom of the first limestones with the first occurrence of *S. isolatus* in the lowermost part of the second cyclothem in the Taiyuan Formation (Fig. 2). Taking together, our conodont fossils could constrain a late Gzhelian (~301–299 Ma) age for the lowest Taiyuan Formation in the Henan Province.

This conodont biostratigraphic constraint for the lowest Taiyuan Formation is slightly older than that previously constrained by fusulinids which were considered to indicate an Early Permian age (Song et al., 2014; Jiang et al., 2002; Liang, 1994; Zhang and Xia, 1985), but is broadly consistent with that constrained by foraminiferal and ostracod biostratigraphy (Song et al., 2021; Li et al., 2013; Zhang and Liang, 1987; Zheng, 1987). This new biostratigraphic constraint for the lowest Taiyuan Formation is in agreement with the recently reported high-precision zircon U-Pb ages of 301.13 ± 0.21 Ma for a tuffaceous claystone bed immediately below the bottom limestones of the Taiyuan Formation and of 299.32 ± 0.14 Ma for a crystalline-lithic tuff from the lower Taiyuan Formation in eastern Henan Province (Yang J H et al., 2020). It is also consistent with a high precision zircon U-Pb age of 298.925 ± 0.073 Ma for a bentonite from the middle Taiyuan Formation of Palougou Section in Shanxi Province (Wu Q et al., 2021), constraining a Gzhelian age for the underlying limestone interval containing conodonts of *Streptognathodus oppletus*, *S. elegantulus*, and *Idiognathodus hebeiensis* (Kong et al., 1996; Wan and Ding, 1987).

3.2 Implications for a Great Sea-Level Rise in the Latest Carboniferous in North China

Based on the sampled successions, the conodont fauna displays a predominance in *Streptognathodus* elements with a few *Idiognathodus* in the bottom limestones of the Taiyuan Formation. Such a conodont fauna has also been reported from the Miaogou limestones and other biostratigraphically correlated limestones of the lowest Taiyuan Formation in Shanxi, Hebei, eastern Shandong, southern Liaoning, Anhui and Jiangsu provinces (Fig. 5; Lang, 2010; Su et al., 2006; Gao et al., 2005; Wang and Qi, 2003; Jiang et al., 2002; Jia et al., 1994; Wang, 1991; Lin and Mao, 1990; Zhang, 1990; Liang, 1989; Zhang et al., 1988; Wan and Ding, 1987, 1984; Wang and Li, 1984; Wan et al., 1983; Zhao and Wan, 1983). Therefore, limestones with a late Gzhelian age in the lowest Taiyuan Formation, such as the studied ones in Wenwan and Baipohe sections, could be widely distributed across North China (Figs. 4 and 5). In the Taiyuan Formation, the limestones have long been considered to represent periodic marine transgressions (Zhang, 1989). Limestones containing conodonts *Neognathodus roundyi*-*Streptognathodus cancellosus*, *Idiognathodus shanxiensis*-*Neognathodus bassleri* and *I. corrugatus*-*I. sinuatus* assemblage can be found in the Benxi Formation in northern North China, suggesting a middle Pennsylvanian age (e.g., Shanxi Province, Pei, 2004, 1999; Wan and Ding, 1987), but are poorly developed in southern North China (e.g., Henan Province, Pei, 1999; Liang, 1989). The limestones of Benxi Formation are confined to the northern North China, while the limestones of Taiyuan Formation

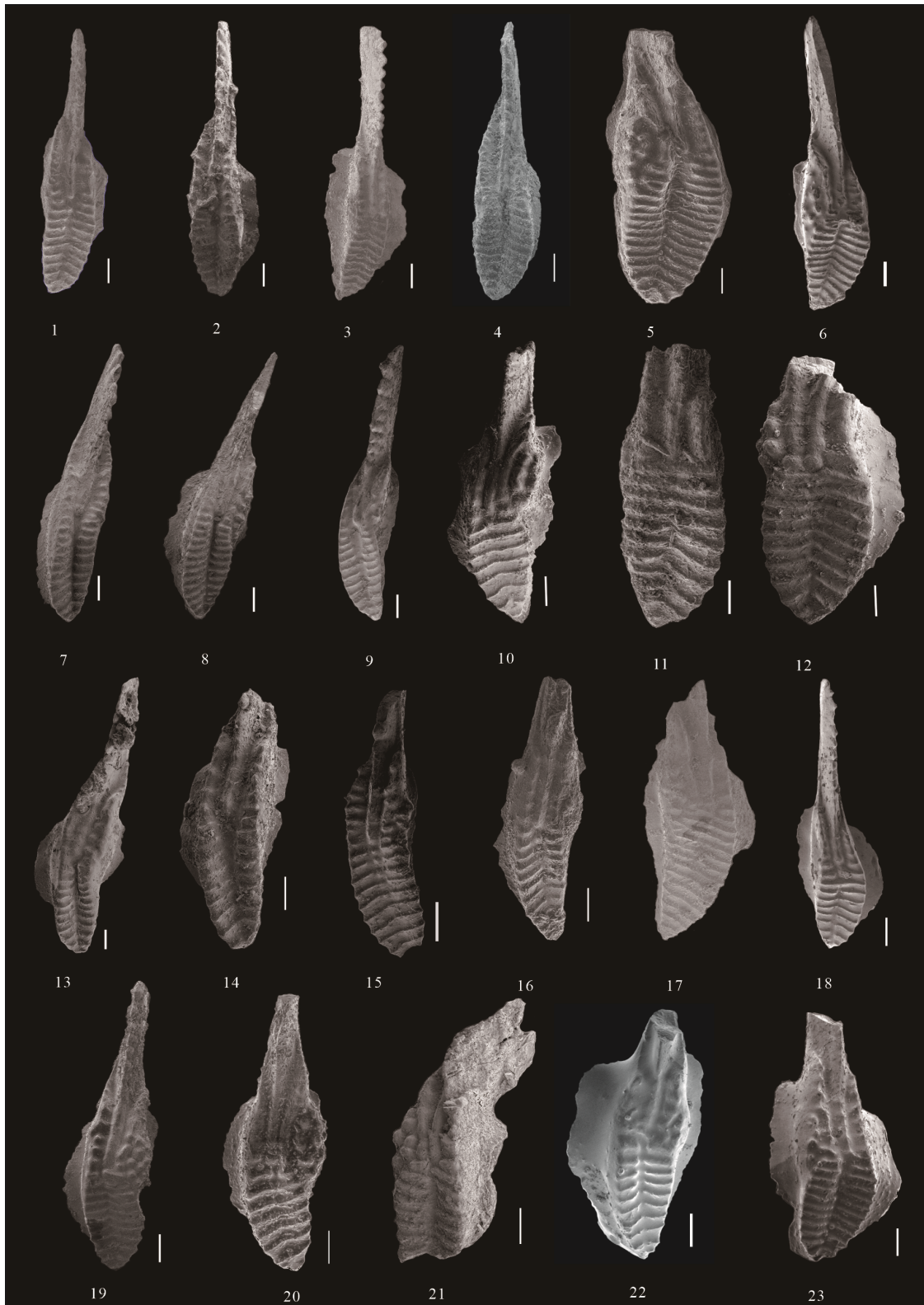


Figure 3. Conodonts from Taiyuan Formation in the Baipohe and Wenwan sections, Henan Province. 1. *Streptognathodus bellus* Chernykh & Ritter, 1997, WW19T-1-4; 2. *S. acuminatus* Gunnell, Chernykh & Reshetkova, 1987, WW19T-1-3; 3. *S. cf. longus* Chernykh, 2005, WW19T-2-13; 4. *S. fuchengensis* Zhao, 1981, MJ19T-4-16; 5–6. *S. isolatus* Chernykh, Ritter & Wardlaw, 1997, MJ19T-4-1, BPH19T-7-2; 7. *S. cf. recreatus* Chernykh, 2005, WW18T-8-2; 8. *S. cf. cristellaris* Chernykh & Reshetkova, 1987, WW18T-8-3; 9. *S. invaginatus* Reshetkova & Chernykh, 1986, WW18T-8-7; 10–12. *Idiognathodus hebeiensis* Zhao & Wan, 1984, DSH18T-1-13, BPH18T-1-035, BPH18T-1-034; 13. *S. nodulinear* Reshetkova and Chernykh, 1986, BPH18T-8-4; 14–16. *S. elongatus* Gunnell, 1933, BPH18T-1-8, BPH18T-3-1, WW19T-2-41 17. *Streptognathodus* sp., WW19T-3-11; 18. *S. conjunctus* Barskov, Isakova & Shchastlivceva, 1981, BPH19T-8-022; 19–21. *S. wabaunsensis* Gunnell, 1933, WW19T-3-8, BPH19T-2-045, BPH19T-3-024; 22. *S. glenisteri* Chernykh & Ritter, 1997, BPH19T-8-021; 23. *S. binodosus* Wardlaw, Boardman & Nestell, 2009, BPH19T-6-002. Scale bars = 100 μ m.

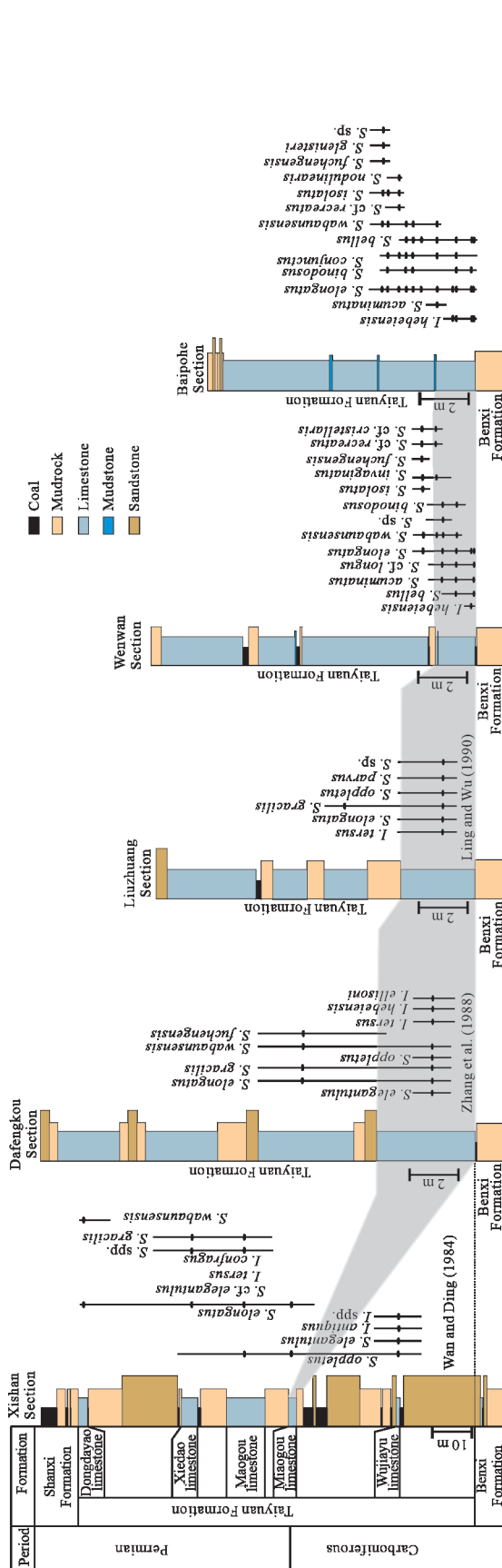


Figure 4. Stratigraphic correlation of the bottom limestones of Taiyuan Formation in southern North China (Dafengkou, Liuzhuang, Wenwan and Baipohe sections in Henan Province) with the Miaogou limestone of Taiyuan Formation in northern North China (Xishan Section in Shanxi Province). The correlation is based on conodont biostratigraphy (Wang and Qi, 2003; Lin and Mao, 1990; Zhang et al., 1988; Wan and Ding, 1987, 1984; this study).

containing a mixed *Idiognathodus hebeiensis* and *Streptognathodus* conodont fauna are widely distributed in North China (Fig. 5). It suggests that the studied limestones would signify a transgression in North China during the Latest Carboniferous and suggest a great sea-level rise during the Latest Carboniferous (301–299 Ma, Fig. 6; Li et al., 1999; Zhong and Fu, 1998).

Relative sea-level changes may result from combinations of several different mechanisms, such as tectonism (basin subsidence and uplift), sediment supply and climate change (Pitman and Golovchenko, 1983). Regional basement subsidence may explain the overall sea-level high in North China which is temporally correlated with sea-level low in both North America and South China during the Asselian (Fig. 6). However, the late Pennsylvanian–Early Permian is also an interval of high-frequency sea level changes. The magnitude of global sea level change could be as high as 100–120 m signifying the acme of the Late Paleozoic Ice Age (Rygel et al., 2008). In U.S. Mid-continent the large-scale relative sea-level fluctuations have been related to large-scale, short-term glacial cycles of waxing and waning of ice sheets (Fig. 6; Heckel, 2008). A late Gzhe-lian rapid transgression has also been suggested from South China (Liu et al., 2017). During this period, glacial deposits recorded a Gondwana-wide deglacial transgression in high latitudes (Griffis et al., 2019, 2018; Fielding et al., 2008; Stollhofen et al., 2008; Scheffler et al., 2003). Such sea-level rise might be associated with a climate warming as documented by a bioherm in Timor and western Australian (Davydov and Biakov, 2015; Davydov, 2013) and by the low brachiopod $\delta^{18}O$ records at the Permo-Carboniferous transition (Grossman and Joachimski, 2020). It is therefore that the bottom limestones of the Taiyuan Formation in southern North China could correspond to a significant global sea-level rise and climate warming event in the Permo-Carboniferous icehouse.

4 SYSTEMATIC PALEONTOLOGY

Illustrated specimens are stored at the China University of Geosciences (Wuhan). Only index fossils with stratigraphic significances are described here.

Genus *Idiognathodus* Gunnell, 1931

Type species *Idiognathodus claviformis* Gunnell, 1931

Idiognathodus hebeiensis Zhao & Wan, 1984

Figures 3.10–3.12

1984 *Idiognathodus hebeiensis* Zhao & Wan n. sp: pl. 108, figs. 1–4, 7–9.

1989 *Idiognathodus hebeiensis* Zhao & Wan: Zhao, pl. 156, fig. 1.

Diagnosis: An asymmetrical Pa element, triangular platform outline, transverse ridges continuous, well-developed nodose lobes on inner sides of the platform.

Description: The Pa elements are slightly to strongly asymmetrical. The dextral element has a more triangular shape with the greatest width on the dorsal part of the platform. The carina is long and slightly constricted with adcarinal ridge, transverse ridges continuous. The sinistral element is elongate and slender, the carina relative shorter, transverse ridges always continuous with shallow trough in posterior. Termination

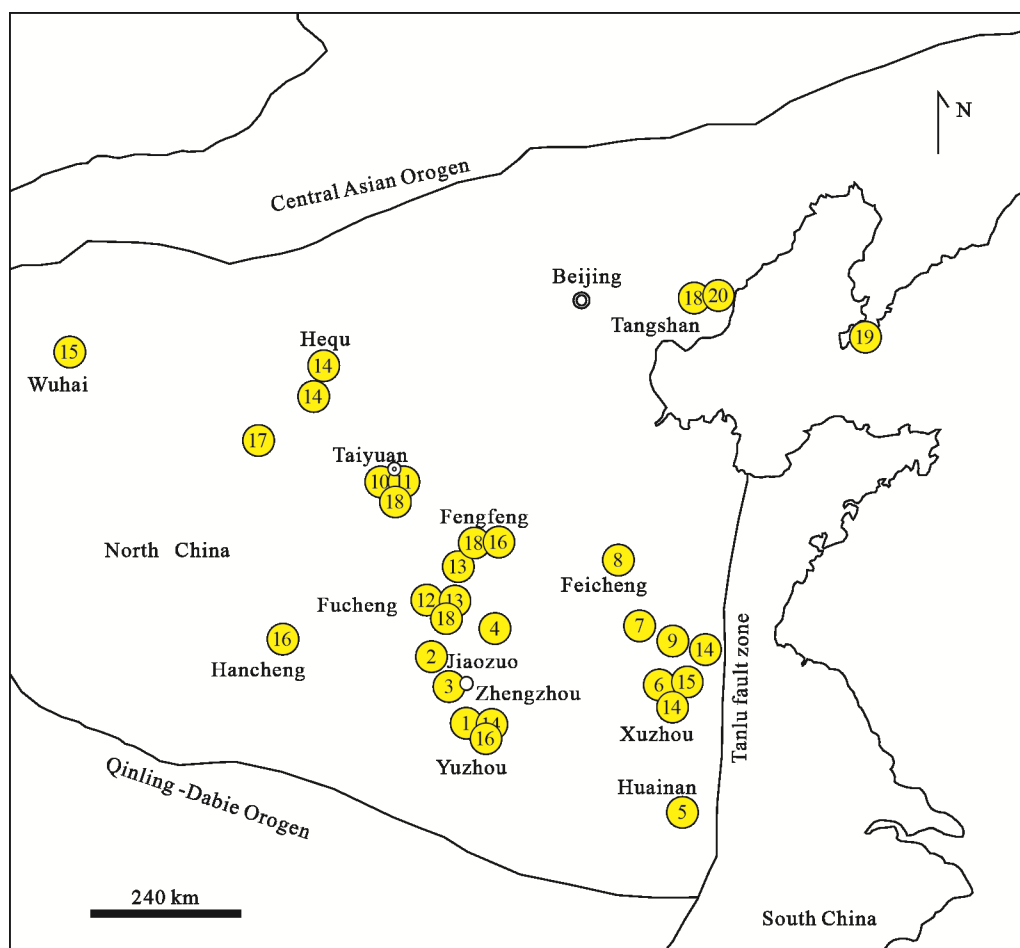


Figure 5. Sketch map showing the distribution of limestones with a mixed *Idiognathodus* and *Streptognathodus* conodont fauna in the lower part and a *Streptognathodus* dominant conodont fauna in the upper part across North China. 1. Zhang et al. (1988); 2. Lin and Mao (1990); 3. Zhang (1990); 4. Liang (1989); 5. Jia et al. (1994); 6. Gao et al. (2005); 7. Jiang et al. (2002); 8. Su et al. (2006); 9. Liu and Liu (1988); 10. Wang and Li (1984); 11. Wan and Ding (1984); 12. Zhao (1981); 13. Wang and Weng (1987); 14. Wan and Ding (1987); 15. Gao et al. (1999); 16. Wang and Qi (2003) 17. Zhang et al. (2018); 18. Wan et al. (1983); 19. Lang (2010); 20. Zhao and Wan (1983).

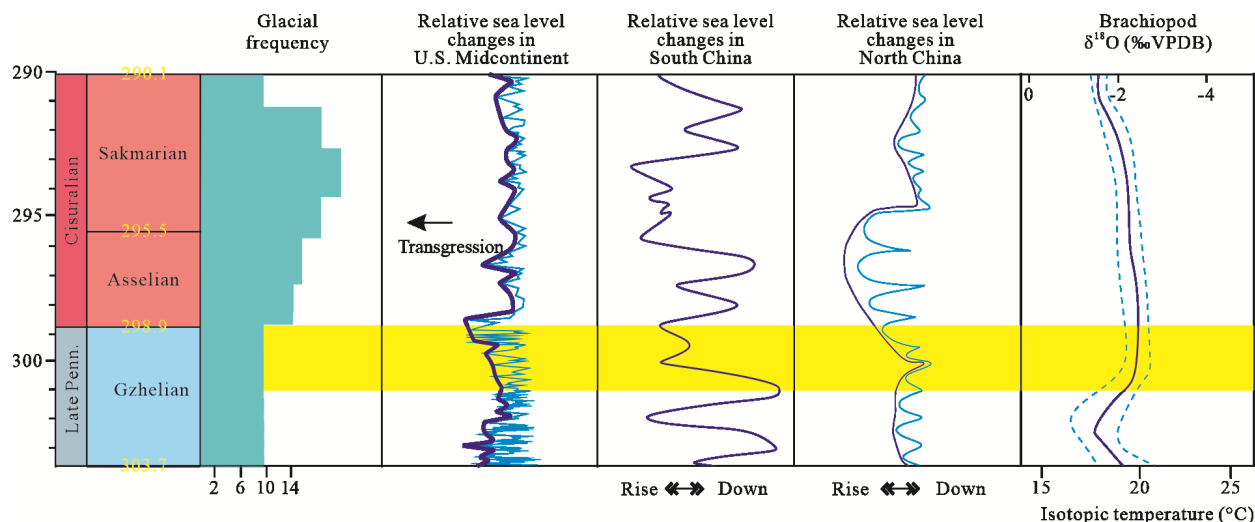


Figure 6. Diagram illustrating the evolution of glaciation history and sea-level fluctuation during the late Pennsylvanian to Early Permian. Glacial frequency and area of glaciation are adapted from Montañez and Poulsen (2013). Relative sea-level changes in U.S. Midcontinent are modified from Heckel (2008), Boardman et al. (2009) and Schmitz and Davydov (2012). Relative sea-level changes in South China and North China are from Liu et al. (2017) and Li et al. (1999), respectively. Brachiopod δ¹⁸O curve from Grossman and Joachimski (2020). Yellow bar marks the age range of ~300–299 Ma for the significant sea-level high in the Latest Carboniferous.

of platform slightly pointed.

Remarks: *Idiognathodus hebeiensis* have been reported in bottom part of Taiyuan Formation in North China. It differs from *I. delicatus* by nodose lobes only on inner sides. It differs from *I. antiquus* by relatively longer platform and well-developed adcarinal ridge.

Occurrences: Gzhelian stage, Taiyuan Formation (most frequently in its basal parts), North China.

Genus *Streptognathodus* Stauffer & Plummer, 1932

Type species *Streptognathodus excelsus* Stauffer & Plummer, 1932.

Streptognathodus acuminatus Gunnell, 1933

Figure 3.2

1933 *Streptognathodus acuminatus* Gunnell, n. sp.: pl. 33, fig. 33.

1987 *Streptognathodus acuminatus* Gunnell: Chernykh and Reshetkova, pl. 7, fig. 5.

1997 *Streptognathodus acuminatus* Gunnell: Chernykh and Reshetkova, Chernykh and Ritter, fig. 6.2.

2012 *Streptognathodus acuminatus* Gunnell: Chernykh and Reshetkova, Chernykh, pl. 19, figs. 6–8.

2017 *Streptognathodus acuminatus* Gunnell: Wang et al., fig. 3.V.

Diagnosis: A species of *Streptognathodus* characterized by an elongate outline, straight and symmetrical platform, shallow median trough, and nearly continuous transverse ridge.

Description: The Pa element that is straight and symmetrical, the widest generally on the middle of posterior platform. The carina termination is gradually fused but does not join to each side of parapet. One to three inner accessory nodes differentiated from posterior of inner adcarinal parapet, a distinct trough between the fused to partially fused adcarinal parapet and the posterior platform parapet. Shallow and narrow median trough, transverse ridges are symmetrical and some crossing for median groove in posterior termination of platform.

Remarks: *Streptognathodus acuminatus* is distinguished from *S. wabaunsensis* by present a distinct trough between the adcarinal parapet and the posterior platform parapet.

Streptognathodus bellus Chernykh & Ritter, 1997

Figure 3.1

1997 *Streptognathodus bellus* Chernykh and Ritter, n. sp.: figs. 4.1–4.8, 4.10.

2005 *Streptognathodus bellus* Chernykh and Ritter: Chernykh, pl. 7, figs. 13–16.

2009 *Streptognathodus bellus* Chernykh and Ritter: Boardman et al., pl. 2, figs. 1, 11; p. 3, fig. 9.

2012 *Streptognathodus bellus* Chernykh and Ritter: Chernykh, pl. 16, figs. 1–17.

Diagnosis: A species of *Streptognathodus* characterized by a relatively robust Pa element with slight asymmetrical and elongate platform, moderately deep to very shallow V-shaped trough, and relatively long transverse ridges for the most of the length of the platform.

Description: The Pa elements with slightly asymmetrical, elongate or relatively robust platform, are widest on the posterior of carina termination. Posterior termination of platform is

pointed to slightly rounded. Transverse ridges extend for most of the platform and crisscrossing. The free blade generally increases in size anteriorly, the carina flanked by slightly serrate or ridged parapets of equal length occupying anterior one-third of platform. The posterior of carina is gradually fused, compressed, and one to three discrete denticles or nodes may occur just posterior of carina termination. The depth of V-shaped media trough ranges from moderately deep to very shallow.

Remarks: *Streptognathodus bellus* differs from *S. elongatus* by longer carina, crossing transverse ridges and more asymmetrical platform.

Streptognathodus binodosus Wardlaw, Boardman & Nestell, 2009

Figure 3.23

2009 *Streptognathodus binodosus* Wardlaw, Boardman & Nestell, n. sp.: pl. 10, figs. 2–6, 8–11; pl. 11, figs. 1, 3–5, 7, 10, 12; pl. 13, fig. 3; pl. 19, figs. 9, 11.

Diagnosis: A species of *Streptognathodus* characterized by a Pa element that has at least one pair of denticles in a transverse row on the inner side immediately to the posterior termination of the carina.

Description: The Pa elements with relatively broad symmetrical or slightly asymmetrical platform, are widest from the posterior of carina termination to middle part of platform. Posterior termination of platform slightly rounded. One pair of laterally arranged denticles in a transverse row behind the posterior termination of the carina. Moderate length of carina with ridge-like or comprised of hemispherical nodes on the posterior of carina. The termination of carina present ‘J’ pattern and extension to the parapet. Parapets of roughly equal length and serrate with small nodes. Median groove is deep anteriorly and becomes narrow posteriorly. One or two transverse ridges merge and cross the groove.

Remarks: *Streptognathodus binodosus* differs from *S. nodulinearioris* by ‘J’ pattern of the carina extension to the parapet. It differs from *S. farmeri* by aligned accessory nodes forming denticle pairs.

Streptognathodus cf. cristellaris Chernykh & Reshetkova, 1987

Figure 3.8

1987 *Streptognathodus cristellaris* Chernykh & Reshetkova, n. sp.: pl. 1, figs. 9–11.

1997 *Streptognathodus cristellaris* Chernykh & Reshetkova: Chernykh and Ritter, figs. 6.1, 6.3–6.6.

2006 *Streptognathodus cristellaris* Chernykh & Reshetkova: Chernykh, pl. 4, figs. 6–8, 14, 15; pl. 5, figs. 19–22.

2009 *Streptognathodus cristellaris* Chernykh & Reshetkova: Boardman et al., pl. 1, figs. 9–11.

2017 *Streptognathodus cristellaris* Chernykh & Reshetkova: Wang et al., fig. 3.5.

Diagnosis: A species of *Streptognathodus* characterized by elongate platform, inner accessory lobes are generally ornamented with elongate ridges. Outer parapet rises slightly above interior of the middle part of the platform. Anterior branches of parapets descends sharply and separate from the free blade by a smooth trough. Median trough is straight and smooth, pass-

ing to posterior end of platform.

Description: The elongate Pa elements with symmetrically located median groove. Posterior termination of platform bluntly pointed. Moderate length of carina termination is gradually fused. Inner high parapet extends to anteriorly further than outer parapet. Lateral accessory lobes are generally ornamented with ribbed nodes, which are merged with the parapet. Transverse ridges are nearly symmetrical and do not cross the median groove.

Remarks: *Streptognathodus cf. cristellaris* differs from *S. wabaunsensis* by reduction in number of nodes and ornamented with elongate ridges in accessory lobes. It differs from *S. fusus* by the presence of accessory nodes.

Occurrences: Asselian stage of the Lower Permian, zone of *S. cristellaris*; China, southern Urals, South Korea.

Streptognathodus fuchengensis Zhao, 1981

Figure 3.4

1981 *Streptognathodus fuchengensis* Zhao, n. sp.: pl. 3, figs. 1, 2.

2009 *Streptognathodus fuchengensis* Zhao, Boardman et al., pl. 12, figs. 5–7; pl. 13, fig. 6; pl. 15, fig. 12; pl. 16, fig. 4.

Diagnosis: A species of *Streptognathodus* characterized by robust Pa element with straight transverse ridges. Narrow median trough. No accessory lobe on the inner side of adcarinal parapet.

Description: The Pa elements with moderate to long platform, are widest in dextral forms on the middle of posterior platform. The free blade generally increasing in size anteriorly, the carina termination is gradually fused, compressed that may extend most of the platform. No accessory denticles developed near to carina. The highest part of platform is near to the posterior of carina termination. Narrow median trough and the deepest and widest of the median trough is near to the carina. Transverse ridge straight, nearly symmetrical and do not cross the median trough. Transverse ridges gradually shorten along platform, are longest at the 1/3 posterior platform. The anterior-most of ridges break up partially into denticles. Inner adcarinal parapet extends to anteriorly further than outer parapet.

Remarks: *Streptognathodus fuchengensis* differs from *S. wabaunsensis* by no accessory lobe on the inner side of adcarinal parapet. It differs from *S. conjunctus* by undisrupted groove posterior and no fused denticles on parapet adjacent to the carina.

Streptognathodus glenisteri Chernykh & Ritter, 1997

Figure 3.22

1997 *Streptognathodus glenisteri* Chernykh & Ritter, n. sp.: figs. 7.7, 7.8, 7.12–7.15.

2006 *Streptognathodus glenisteri* Chernykh & Ritter: Chernykh, pl. 3, figs. 16–18.

Diagnosis: A species of *Streptognathodus* characterized by an asymmetrical platform with outwardly deflected carina. The anterior of median groove is almost occluded.

Description: The Pa element with moderate to long, asymmetrical platform, carina short and outwardly deflected to outer parapet. Posterior of carina termination is comprised of hemispherical nodes and may gradually merged into adcarinal parapet. Inner lobe bears one or more nodes. Median trough oc-

cluded or reduced to a narrow slit immediately to the posterior carina. Transverse ridges parallel to each other and cross the posterior median trough. Posterior termination of platform slightly bluntly pointed.

Remarks: *Streptognathodus glenisteri* considered as a transitional element from *S. isolatus* to *S. cristellaris*, it differs from *S. isolatus* by an obvious outwardly deflected carina. *S. glenisteri* differs from *S. cristellaris* by a reduction in the number of nodes on the inflated accessory lobe.

Streptognathodus cf. longus Chernykh, 2005

Figure 3.3

2005 *Streptognathodus longus* Chernykh, n. sp.: pl. 7, figs. 1–12; pl. 12, figs. 10, 15.

2006 *Streptognathodus latus* Chernykh: Chernykh, pl. 6, figs. 10–12, 14, 15

2012 *Streptognathodus longus* Chernykh: Chernykh, pl. 16, figs. 18–20; pl. 19, figs. 16–18.

Diagnosis: A species of *Streptognathodus* characterized by a elongate and symmetrical Pa element, transverse ridges partly cross the median groove.

Description: The Pa element with a slender, elongate and symmetrical platform. Posterior termination of platform bluntly pointed.

The carina is moderate in length, the posterior of carina termination is gradually fused or formed one or two discrete denticle. Outer parapet is shorter than the inner parapet. Tiny nodes developed in lateral inner parapet. Median trough is shallow and narrow, are deepest near to posterior termination of the carina. Transverse ridge straight and continuous from middle to posterior of platform.

Remarks: *Streptognathodus longus* differs from *S. elongatus* by flat and more narrowly platform. It differs from *S. bellus* by symmetrical platform and not obvious median trough.

Streptognathodus isolatus Chernykh, Ritter & Wardlaw, 1997

Figures 3.5–3.6

1997 *Streptognathodus isolatus* Chernykh, Ritter, and Wardlaw, n. sp.: pls. 162–164, figs. 4, 5, 6, 7–8, 11–13, 15.

2003 *Streptognathodus isolatus* Chernykh, Ritter, and Wardlaw: Wang and Qi, pl. 1, figs. 10, 11, 19.

2005 *Streptognathodus isolatus* Chernykh, Ritter, and Wardlaw: Chernykh, pl. 5, figs. 1–6; pl. 6, figs. 1–5.

2006 *Streptognathodus isolatus* Chernykh, Ritter, and Wardlaw: Chernykh, pl. 1, figs. 4–7; pl. 5, fig. 1.

2009 *Streptognathodus isolatus* Chernykh, Ritter, and Wardlaw: Boardman et al., pl. 12, figs. 3, 4, 10; pl. 13, figs. 1, 8, 10–12; pl. 15, figs. 7–9; pl. 19, fig. 7.

2017 *Streptognathodus isolatus* Chernykh, Ritter, and Wardlaw: Wang et al., figs. 3. L, N, P–T.

Diagnosis: Pa element with well-developed inner accessory lobe. A narrow and nodes separated by shallow trough from remainder of platform. Inner adcarinal parapet partially fused with the posterior platform parapet.

Description: The Pa element with symmetrical, elongate or robust platform, are widest on anterior part of posterior platform. The dextral element has a more robust shape with slight-

ly rounded posterior termination of platform. The sinistral element is elongate and slender with pointed posterior termination of platform. The free blade generally increases in size anteriorly. Carina is short, the posterior of carina termination is gradually fused or to discrete denticle. The termination of the carina occasionally submerge into transverse denticles or fused adcarinal parapet. Narrow median trough, the widest and deepest part of median groove is near the carina. Transverse ridges are symmetrical but hardly cross the median groove.

Remarks: As a standard fossil for the division of Carboniferous to Permian boundary, *Streptognathodus isolatus* were marked by its isolated lobe, which is separated by a moat-like trough from the carina. *S. glenisteri* maybe as descend of *S. isolatus* by carina deflection and near occluded anterior trough.

Occurrences: Asselian stage of the Lower Permian, zone of *S. isolatus*; China, North American Midcontinent, southern Urals, South Korea.

Streptognathodus wabaunsensis Gunnell, 1933

Figures 3.19–3.21

1933 *Streptognathodus wabaunsensis* Gunnell, n. sp.: pl. 33, fig. 32.

1997 *Streptognathodus wabaunsensis* Gunnell: Chernykh and Ritter, figs. 6.8–6.12.

2006 *Streptognathodus wabaunsensis* Gunnell: Chernykh, pl. 1, figs. 1–3.

2009 *Streptognathodus wabaunsensis* Gunnell: Boardman et al., pl. 5, figs. 1–7, 9–10; pl. 7, figs. 1–2, 5, 8–9; pl. 8, figs. 5–7; pl. 9, fig. 4; pl. 19, fig. 10.

2012 *Streptognathodus wabaunsensis* Gunnell: Chernykh, pl. 19, figs. 2–5, 9–15; pl. 10, figs. 1–18.

2017 *Streptognathodus wabaunsensis* Gunnell: Wang et al., fig. 3. M.

Diagnosis: Pa element with inner accessory denticles, shallow and narrow median trough, adcarinal parapets do not join the posterior transverse denticles.

Description: The Pa elements with slightly to strongly asymmetrical, robust platform, are widest on the posterior of termination of carina. Posterior termination of platform pointed to slightly rounded. The free blade generally increases in size anteriorly, the carina short and carina termination is gradually fused or to discrete denticle. Adcarinal parapets do not join the posterior of either transverse denticles or carina termination. Shallow and narrow median trough, transverse ridges are symmetrical and some cross the median trough.

Remarks: *Streptognathodus wabaunsensis* is distinguished from *S. nodulinearis* by latter has a linear arrangement of accessory nodes. The difference among this species and *S. isolatus* by latter has a shallow trough separated from the remainder of platform.

Occurrences: Gzhelian stage of the Upper Carboniferous, zone of *S. wabaunsensis*, China, North American Midcontinent, southern Urals, South Korea.

5 CONCLUSIONS

We conducted a conodont biostratigraphy study in two sections to constrain the age of the lower Taiyuan Formation in southern North China. There is a *Streptognathodus* dominated

conodont assemblage in the lower limestones of the Taiyuan Formation in the Wenwan and Baipohe sections. Combined with previously reported high-precision zircon U-Pb zircon ages, the lowest Taiyuan Formation can be constrained confidently in the Latest Carboniferous in Henan Province. Based on our conodont fauna, the bottom limestones of the Taiyuan Formation in Henan Province could be bio-stratigraphically correlated with the Miaogou limestones and other correlative limestones of the lower Taiyuan Formation in Shanxi Province and many other regions, suggesting a significant pan-North China transgression in the late Gzhelian. This marine transgression in North China could be correlated with that reported from South China, North America, Russia and Gondwana continents. It is suggested that the bottom limestones of the Taiyuan Formation in southern North China could correspond to a global sea-level rise and a significant deglacial warming in the Permo-Carboniferous icehouse.

ACKNOWLEDGMENTS

This study was supported by the National Natural Science Foundation of China (Nos. 41572078, 41872106, 42072013), and the BGEG and GPMR laboratory funds (Nos. GKZ18Y660, GPMR201609). The final publication is available at Springer via <https://doi.org/10.1007/s12583-021-1526-8>.

REFERENCES CITED

- Alekseev, A. S., Goreva, N. V., 2007. Conodont Zonation for the Type Kasimovian and Gzhelian Stages in the Moscow Basin, Russia. In: Wong, T. E., ed., Proceedings of the XVth International Congress on Carboniferous and Permian Stratigraphy. Royal Netherlands Academy of Arts and Sciences, Utrecht. 229–242
- Barrick, J. E., Lambert, L., Heckel, P., et al., 2013. Midcontinent Pennsylvanian Conodont Zonation. *Stratigraphy*, 10(1/2): 55–72
- Boardman, D. R. I. I., Wardlaw, B. R., Nestell, M. K., 2009. Stratigraphy and Conodont Biostratigraphy of Uppermost Carboniferous and Lower Permian from North American Midcontinent. *Kansas Geological Survey Bulletin*, 255: 1–253
- Chernykh, V. V., Reshetkova, N. P., 1987. Biostratigraphy and Conodonts of the Carboniferous and Permian Boundary Beds of the Western Slope of the Southern and Central Urals. Urals Scientific Center of the USSR Academy of Sciences, Sverdlovsk. 45 (in Russian)
- Chernykh, V. V., Ritter, S. M., 1997. *Streptognathodus* (Conodonta) Succession at the Proposed Carboniferous-Permian Boundary Stratotype Section, Aidaralash Creek, Northern Kazakhstan. *Journal of Paleontology*, 71(3): 459–474. <https://doi.org/10.1017/s002233600039470>
- Chernykh, V. V., Ritter, S. M., Wardlaw, B. R., 1997. *Streptognathodus isolatus* New Species (Conodonta): Proposed Index for the Carboniferous-Permian Boundary. *Journal of Paleontology*, 71(1): 162–164. <https://doi.org/10.1017/s002233600039068>
- Chernykh, V. V., 2002. Zonal Scale of the Gzhelian and Kasimovian Stages Based on Conodonts of the Genus *Streptognathodus*. In: Chuvashov, B. L., Amon, E. A., eds., Stratigraphy and Paleogeography of Carboniferous of Eurasia. Nauka, Ekaterinburg. 302–306 (in Russian)
- Chernykh, V. V., 2005. Zonal Method of Biostratigraphy, Conodont Zonal Scale of the Lower Permian of the Urals. The Institute of Geology and Geochemistry, UB RAS, Ekaterinburg. 217 (in Russian)
- Chernykh, V. V., 2006. Lower Permian Conodonts in the Urals. The Institute of Geology and Geochemistry, UB RAS, Ekaterinburg. 130

- (in Russian)
- Chernykh, V. V., 2010. Divergence and the Directed Change of the Pa Element in Conodonts of the Streptognathodus Group. *Litosfera*, 4: 69–80 (in Russian)
- Chernykh, V. V., 2012. Conodonts of Gzhelian Stage of Urals. Institute of Geology and Geochemistry, UB RAS, Ekaterinburg. 158 (in Russian)
- Chernykh, V. V., 2020. General Regularities in the Development Gzhelian-Asselian Conodonts. *Litosfera*, 20(4): 471–485. <https://doi.org/10.24930/1681-9004-2020-20-4-471-485>
- Davydov, V. I., Biakov, A. S., 2015. Discovery of Shallow-Marine Biofacies Conodonts in a Bioherm within the Carboniferous-Permian Transition in the Omolon Massif, NE Russia near the North Paleo-Pole: Correlation with a Warming Spike in the Southern Hemisphere. *Gondwana Research*, 28(2): 888–897. <https://doi.org/10.1016/j.gr.2014.07.008>
- Davydov, V. I., Haig, D. W., McCartain, E., 2013. A Latest Carboniferous Warming Spike Recorded by a Fusulinid-Rich Bioherm in Timor Leste: Implications for East Gondwana Deglaciation. *Palaeogeography, Palaeoclimatology, Palaeoecology*, 376: 22–38. <https://doi.org/10.1016/j.palaeo.2013.01.022>
- Fan, G. Q., 1991. Carboniferous Marine Transgression in North China. *Regional Geology of China*, 10(4): 349–355, 372 (in Chinese with English Abstract)
- Fielding, C. R., Frank, T. D., Birgenheier, L. P., et al., 2008. Stratigraphic Imprint of the Late Palaeozoic Ice Age in Eastern Australia: A Record of Alternating Glacial and Nonglacial Climate Regime. *Journal of the Geological Society*, 165(1): 129–140. <https://doi.org/10.1144/0016-76492007-036>
- Frakes, L. A., Francis, J. E., Syktus, J. I., 1992. Climate Modes of the Phanerozoic. Cambridge University Press, Cambridge. 274. <https://doi.org/10.1017/cbo9780511628948>
- Gao, F., Xu, X. Q., Zhou, G. Q., 1999. The Distribution of Conodonts from Taiyuan Formation and Its Stratigraphic Significance in Xuzhou Area. *Coal Geology of China*, 11(1): 17–19 (in Chinese with English Abstract)
- Gao, L. F., Ding, H., Wan, X. Q., 2005. Taxonomic Revision of Conodont *Sweetognathus* Species in the Uppermost Taiyuan Formation, Yuhuai Basin and Its Significance. *Acta Micropalaeontologica Sinica*, 22(4): 370–382 (in Chinese with English Abstract)
- Goreva, N. V., Alekseev, A. S., 2010. Upper Carboniferous Conodont Zones of Russia and Their Global Correlation. *Stratigraphy and Geological Correlation*, 18(6): 593–606. <https://doi.org/10.1134/s086959381006002x>
- Griffis, N. P., Montañez, I. P., Mundil, R., et al., 2019. Coupled Stratigraphic and U-Pb Zircon Age Constraints on the Late Paleozoic Icehouse-to-Greenhouse Turnover in South-Central Gondwana. *Geology*, 47(12): 1146–1150. <https://doi.org/10.1130/g46740.1>
- Griffis, N. P., Mundil, R., Montañez, I. P., et al., 2018. A New Stratigraphic Framework Built on U-Pb Single-zircon TIMS Ages and Implications for the Timing of the Penultimate Icehouse (Paraná Basin, Brazil). *GSA Bulletin*, 130(5/6): 848–858. <https://doi.org/10.1130/b31775.1>
- Grossman, E. L., Joachimski, M. M., 2020. Chapter 10-Oxygen Isotope Stratigraphy. *Geologic Time Scale 2020*. Elsevier, Amsterdam. 279–307. <https://doi.org/10.1016/b978-0-12-824360-2.00010-3>
- Gunnell, F. H., 1933. Conodonts and Fish Remains from the Cherokee, Kansas City, and Wabausee Groups of Missouri and Kansas. *Journal of Paleontology*, 7(3): 261–297
- Gunnell, F. H., 1931. Conodonts from the Fort Scott Limestone of Missouri. *Journal of Paleontology*, 5(3): 244–252
- Heckel, P. H., Alekseev, A. S., Barrick, J. E., et al., 2007. Cyclothem [“Digital”] Correlation and Biostratigraphy across the Global Moscovian-Kasimovian-Gzhelian Stage Boundary Interval (Middle-Upper Pennsylvanian) in North America and Eastern Europe. *Geology*, 35(7): 607–610. <https://doi.org/10.1130/g23564a.1>
- Heckel, P. H., 1994. Evaluation of Evidence for Glacio-Eustatic Control over Marine Pennsylvanian Cyclothem in North America and Consideration of Possible Tectonic Effects. Tectonic and Eustatic Controls on Sedimentary Cycles. *SEPM Society for Sedimentary Geology*, 4: 65–87. <https://doi.org/10.2110/csp.94.04.0065>
- Heckel, P. H., 2008. Pennsylvanian Cyclothem in Midcontinent North America as Far-Field Effects of Waxing and Waning of Gondwana Ice Sheets. In: Fielding, C. R., Frank, T. D., Isbell, J. L., eds., Resolving the Late Paleozoic Ice Age in Time and Space. *GSA Special Publication*, 441: 275–289. [https://doi.org/10.1130/2008.2441\(19\)](https://doi.org/10.1130/2008.2441(19))
- Heckel, P., Alekseev, A., Barrick, J. E., et al., 2005. Cyclothem [Sequence Stratigraphic] Correlation and Biostratigraphy across the Moscovian-Kasimovian and Kasimovian-Gzhelian Stage Boundaries (Upper Pennsylvanian Series) in North America and Eurasia. *Newsletter on Carboniferous Stratigraphy*, 23: 36–44
- Henderson, C. M., 2018. Permian Conodont Biostratigraphy. *Geological Society, London, Special Publications*, 450(1): 119–142. <https://doi.org/10.1144/sp450.9>
- Hogancamp, N. J., 2020. P1 Element Morphological Variability within the Late Pennsylvanian Asymmetrical Idiognathodus Clade from the Midcontinent, USA and Implications for Ontogeny, Taxonomy, Phylogeny, and Function. *Palaeogeography, Palaeoclimatology, Palaeoecology*, 549: 109090. <https://doi.org/10.1016/j.palaeo.2019.02.016>
- Hu, K. Y., Qi, Y. P., Qie, W. K., et al., 2020. Carboniferous Conodont Zonation of China. *Newsletters on Stratigraphy*, 53(2): 141–190. <https://doi.org/10.1127/nos/2019/0498>
- Huang, D. M., Dong, C. Y., Wan, Y. S., 2020. Late Neoproterozoic-Late Paleoproterozoic Magmato-Tectonothermal Events in the Xiaojinling Area, Southern Margin of the North China Craton, as Documented by Zircon U-Pb-Hf Isotope Analyses and Whole-Rock Geochemistry. *Earth Science*, 45(9): 3330–3340. <https://doi.org/10.3799/dqkx.2020.132> (in Chinese with English Abstract)
- Isbell, J. L., Lenaker, P. A., Askin, R. A., et al., 2003. Reevaluation of the Timing and Extent of Late Paleozoic Glaciation in Gondwana: Role of the Transantarctic Mountains. *Geology*, 31(11): 977–980. <https://doi.org/10.1130/g19810.1>
- Jia, Y. Y., Ding, H., Zhang, W. M., 1994. The Taiyuan Formation Conodont Biostratigraphy of Huainan Coalfield. *Shanxi Mining Institute Learned Journal*, 12(2): 133–142 (in Chinese with English Abstract)
- Jiang, H. C., Zhang, X. Q., Wang, M. Z., et al., 2002. Conodont Biostratigraphy in Taiyuan and Benxi Formations from the Jining Coalfield (East Area), Shandong. *Journal of Stratigraphy*, 26(1): 27–32, 38 (in Chinese with English Abstract)
- Joeckel, R. M., 1994. Virgilian (Upper Pennsylvanian) Paleosols in the Upper Lawrence Formation (Douglas Group) and Its Snyderville Shale Member (Oread Formation, Shawnee Group) of the Northern Midcontinent, USA; Pedologic Contrasts in a Cyclothem Sequence. *Journal of Sedimentary Research*, 64(4): 853–866. <https://doi.org/10.1306/d4267ec7-2b26-11d7-8648000102c1865d>
- Joeckel, R. M., 1999. Paleosol in Galesburg Formation (Kansas City Group, Upper Pennsylvanian), Northern Midcontinent, USA: Evidence for Climate Change and Mechanisms of Marine Transgression. *Journal of Sedimentary Research*, 69(3): 720–737. <https://doi.org/10.2110/jsr>

- 69.720
- Kong, X. Z., Xu, H. L., Li, R. L., et al., 1996. Late Paleozoic Coal-Bearing Strata and Biota in Shanxi, Taiyuan, China. Science and Technology of Shanxi Press, Taiyuan. 280 (in Chinese)
- Lang, J. B., 2010. Late Carboniferous Conodonts from Southeastern Liaoning and Re-study of the Benxi Formation: [Dissertation]. Jilin University, Changchun. 1–109 (in Chinese with English Abstract)
- Li, B. F., Wen, X. D., Li, G. D., 1999. High Resolution Sequence Stratigraphy Analysis on the Permo-Carboniferous in North China Platform. *Earth Science Frontiers*, 6(S1): 81–94 (in Chinese with English Abstract)
- Li, C. F., Wang, Z. L., Zhou, Y. Q., et al., 2013. Discussion on Taiyuan Formation Foraminiferal Fauna and Permian-Carboniferous Boundary in Hebi Area, Henan. *Coal Geology of China*, 25(11): 11–16 (in Chinese with English Abstract)
- Li, H. Y., He, B., Xu, Y. G., et al., 2010. U-Pb and Hf Isotope Analyses of Detrital Zircons from Late Paleozoic Sediments: Insights into Interactions of the North China Craton with Surrounding Plates. *Journal of Asian Earth Sciences*, 39(5): 335–346. <https://doi.org/10.1016/j.jseae.2010.05.002>
- Li, Z. X., Wei, J. C., Wang, M. Z., et al., 1996. Sequence Stratigraphic Framework and Sea-Level Changes in the Late Palaeozoic Epicontinental Basin in Northern China. *Sedimentary Facies and Palaeogeography*, 16(5): 1–11 (in Chinese with English Abstract)
- Liang, X. Y., 1989. The Preliminary Study of Biostratigraphic Strata in Hebi City, Henan Province. *Coal Geology of China*, 1(2): 12–17 (in Chinese with English Abstract)
- Liang, X. Y., 1994. Fusulinid Zones of the Taiyuan Formation in Yingyang-Gongxian Area, Henan. *Journal of Stratigraphy*, 18(3): 189–195. <https://doi.org/10.19839/j.cnki.dcxz.1994.03.005> (in Chinese with English Abstract)
- Lin, Y. L., Mao, G. Y., 1990. The Conodonts Association and Their Features of Taiyuan Formation from Jiaozuo Area. *Journal of Henan Polytechnic University (Natural Science)*, 9(1): 30–37 (in Chinese with English Abstract)
- Liu, C., Jarochowska, E., Du, Y. S., et al., 2017. Stratigraphical and $\delta^{13}\text{C}$ Records of Permo-Carboniferous Platform Carbonates, South China: Responses to Late Paleozoic Icehouse Climate and Icehouse-Greenhouse Transition. *Palaeogeography, Palaeoclimatology, Palaeoecology*, 474: 113–129. <https://doi.org/10.1016/j.palaeo.2016.07.038>
- Liu, S., Sun, Z. Y., Ji, C., et al., 2020. Conodont Biostratigraphy and Age of the Early Triassic Fish-Bearing-Nodule Levels from Nanjing and Jurong, Jiangsu Province, South China. *Journal of Earth Science*, 31(1): 9–22. <https://doi.org/10.1007/s12583-019-1232-y>
- Liu, Y., Liu, H. F., 1988. Conodonts of Taiyuan Formation in Xulou Area, Tengxian County, Shandong Province and Its Stratigraphic Significance. *Journal of Northwest University (Natural Science Edition)*, 3: 87–88 (in Chinese with English Abstract)
- Lü, D. W., Wei, X. W., Liu, H. Y., et al., 2009. Classification of Paleogeomorphology Units and Law of Coal Accumulation in Late Carboniferous of North China Plate. *Petroleum Geology and Recovery Efficiency*, 17(5): 24–27, 112. <https://doi.org/10.13673/j.cnki.cn37-1359/te.2010.05.028> (in Chinese with English Abstract)
- Montañez, I. P., McElwain, J. C., Poulsen, C. J., et al., 2016. Climate, $p\text{CO}_2$ and Terrestrial Carbon Cycle Linkages during Late Palaeozoic Glacial-Interglacial Cycles. *Nature Geoscience*, 9(11): 824–828. <https://doi.org/10.1038/ngeo2822>
- Montañez, I. P., Poulsen, C. J., 2013. The Late Paleozoic Ice Age: An Evolving Paradigm. *Annual Review of Earth and Planetary Sciences*, 41: 629–656. <https://doi.org/10.1146/annurev.earth.031208.100118>
- Montañez, I. P., Tabor, N. J., Niemeier, D., et al., 2007. CO_2 -Forced Climate and Vegetation Instability during Late Paleozoic Deglaciation. *Science*, 315(5808): 87–91. <https://doi.org/10.1126/science.1134207>
- Pei, F., 1999. Multiple Stratigraphic Division and Correlation of the Permo-Carboniferous of Yuzhou of Henan and Taiyuan of Shanxi. *Regional Geology of China*, 18(2): 132–139, 147 (in Chinese with English Abstract)
- Pei, F., 2004. The North China Type Permo-Carboniferous Fusulinid and Conodont Biostratigraphic Units of Henan Province. *Journal of Stratigraphy*, 28(4): 344–353 (in Chinese with English Abstract)
- Pitman, W. C. III, Golovchenko, X., 1983. The Effect of Sealevel Change on the Shelfedge and Slope of Passive Margins. In: Stanley, D. J., Moore, G. T., eds., *The Shelfbreak: Critical Interface on Continental Margins. SEPM Special Publication*, 33: 41–58. <https://doi.org/10.2110/pec.83.06.0041>
- Reshetkova, N. P., Chernikh, V. V., 1986. New Species of Asselian Conodonts from the Western Slope of the Urals. *Paleontological Journal*, 4: 99–104
- Rygel, M. C., Fielding, C. R., Frank, T. D., et al., 2008. The Magnitude of Late Paleozoic Glacioeustatic Fluctuations: A Synthesis. *Journal of Sedimentary Research*, 78(8): 500–511. <https://doi.org/10.2110/jsr.2008.058>
- Saltzman, M. R., 2003. Late Paleozoic Ice Age: Oceanic Gateway or $p\text{CO}_2$? *Geology*, 31(2): 151–154. [https://doi.org/10.1130/0091-7613\(2003\)0310151:lpiaog>2.0.co;2](https://doi.org/10.1130/0091-7613(2003)0310151:lpiaog>2.0.co;2)
- Scheffler, K., Hoernes, S., Schwark, L., 2003. Global Changes during Carboniferous-Permian Glaciation of Gondwana: Linking Polar and Equatorial Climate Evolution by Geochemical Proxies. *Geology*, 31(7): 605–608. [https://doi.org/10.1130/0091-7613\(2003\)0310605:gdco>2.0.co;2](https://doi.org/10.1130/0091-7613(2003)0310605:gdco>2.0.co;2)
- Schmitz, M. D., Davydov, V. I., 2012. Quantitative Radiometric and Biostratigraphic Calibration of the Pennsylvanian-Early Permian (Cisuralian) Time Scale and Pan-Euramerican Chronostratigraphic Correlation. *Geological Society of America Bulletin*, 124(3/4): 549–577. <https://doi.org/10.1130/b30385.1>
- Shang, G. X., 1997. Late Paleozoic Coal Geology of North China Platform. Shanxi Science and Technology Press, Taiyuan. 1–406 (in Chinese)
- Shen, S. Z., Zhang, H., Zhang, Y. C., et al., 2019. Permian Integrative Stratigraphy and Timescale of China. *Science China Earth Sciences*, 62(1): 154–188. <https://doi.org/10.1007/s11430-017-9228-4>
- Sobolev, N. N., Nakrem, H. A., 1996. Middle Carboniferous-Lower Permian Conodonts of Novaya Zemlya. Norwegian Polar Institute, Oslo. 1–99
- Song, H. B., Hu, B., Zhang, L., et al., 2011. Characteristics of Lithofacies Paleogeography of the Taiyuan Formation Sedimentary Period, Henan Province. *Acta Sedimentologica Sinica*, 29(5): 876–888. <https://doi.org/10.14027/j.cnki.cjxb.2011.05.019> (in Chinese with English Abstract)
- Song, J. J., Song, H. B., Hu, B., 2014. Geologic Age of the Taiyuan Formation in Northwest Henan Province: Evidences from Fusulinids (Foraminifera). *Acta Micropalaeontologica Sinica*, 31(2): 190–204 (in Chinese with English Abstract)
- Song, X. S., Jiang, Y., Chen, J., et al., 2021. Study on Microfossil Assemblage and Age of Xujiashuang Limestone at the Bottom of Taiyuan Formation in Xinwen Coalfield Shandong Province. *Shandong Land and Resources*, 37(1): 19–27 (in Chinese with English Abstract)
- Soreghan, G. S., Soreghan, M. J., Heavens, N. G., 2019. Explosive

- Volcanism as a Key Driver of the Late Paleozoic Ice Age. *Geology*, 47(7): 600–604. <https://doi.org/10.1130/g46349.1>
- Stauffer, C. R., Plummer, H. J., 1932. Texas Pennsylvanian Conodonts and Their Stratigraphic Relations: *University of Texas, Bulletin*, 3201: 13–50
- Stollhofen, H., Werner, M., Stanistreet, I. G., et al., 2008. Single-Zircon U-Pb Dating of Carboniferous-Permian Tuffs, Namibia, and the Intercontinental Deglaciation Cycle Framework. In: Fielding, C. R., Frank, T. D., Isbell, J. L., eds., Resolving the Late Paleozoic Ice Age in Time and Space. *GSA Special Publication*, 441: 83–96. [https://doi.org/10.1130/2008.2441\(06\)](https://doi.org/10.1130/2008.2441(06))
- Su, W., Zhang, J. S., Zhang, X. Q., et al., 2006. Conodonts from the Taiyuan Formation and Benxi Formation in the Feicheng Coalfield, Shandong. *Geological Review*, 52(2): 145–152, 289. <https://doi.org/10.16509/j.georeview.2006.02.001> (in Chinese with English Abstract)
- Tang, K. J., 1989. Lithofacies Paleogeography of North China Platform in Late Paleozoic. *Acta Sedimentologica Sinica*, 7(4): 97–104 (in Chinese with English Abstract)
- Veever, J. J., Powell, C. M., 1987. Late Paleozoic Glacial Episodes in Gondwanaland Reflected in Transgressive-Regressive Depositional Sequences in Euramerica. *GSA Bulletin*, 98(4): 475–487. [https://doi.org/10.1130/0016-7606\(1987\)98475:lpgeig>2.0.co;2](https://doi.org/10.1130/0016-7606(1987)98475:lpgeig>2.0.co;2)
- Wan, S. L., Ding, H., 1984. Preliminary Studies of Carboniferous Conodonts from the Western Mountain, Taiyuan. *Geological Review*, 30(5): 409–415, 511. <https://doi.org/10.16509/j.georeview.1984.05.002> (in Chinese with English Abstract)
- Wan, S. L., Ding, H., 1987. New Discovery in the Study of Permian Carboniferous Conodonts in North China Platform and Its Geological Significance. *Journal of China Coal Society*, 12(1): 13–16, 97 (in Chinese with English Abstract)
- Wan, S. L., Ding, H., Zhao, S. Y., 1983. Middle and Late Carboniferous Conodont Biostratigraphy of North China. *Journal of China Coal Society*, 8(2): 62–72, 100 (in Chinese with English Abstract)
- Wan, Y. S., Xie, H. Q., Dong, C. Y., et al., 2020. Timing of Tectonothermal Events in Archean Basement of the North China Craton. *Earth Science*, 45(9): 3119–3160. <https://doi.org/10.3799/dqkx.2020.121> (in Chinese with English Abstract)
- Wang, J., 2010. Late Paleozoic Macrofloral Assemblages from Weibei Coalfield, with Reference to Vegetational Change through the Late Paleozoic Ice-Age in the North China Block. *International Journal of Coal Geology*, 83(2/3): 292–317. <https://doi.org/10.1016/j.coal.2009.10.007>
- Wang, Q. L., Wang, Y., Qi, Y. P., et al., 2017. Revised Conodont and Fusuline Biostratigraphy of the Bamchi Formation (Pyongan Supergroup) at the Bamchi Section, Yeongwol and the Carboniferous-Permian Boundary in South Korea, Alcheringa: An Australasian. *Journal of Palaeontology*, 42(2): 244–257. <https://doi.org/10.1080/03115518.2017.1395077>
- Wang, X. D., Hu, K. Y., Qie, W. K., et al., 2019. Carboniferous Integrative Stratigraphy and Timescale of China. *Science China Earth Sciences*, 62(1): 135–153 (in Chinese)
- Wang, Z. H., 1991. Conodonts from Carboniferous-Permian Boundary Strata in China with Comments on the Boundary. *Acta Palaeontologica Sinica*, 30: 6–45 (in Chinese with English Abstract)
- Wang, Z. H., Li, R. L., 1984. Discovery of Late Carboniferous Conodonts from Shanxi Province and Its Significance. *Acta Palaeontologica Sinica*, 23(2): 196–203, 271. <https://doi.org/10.19800/j.cnki.aps.1984.02.006> (in Chinese with English Abstract)
- Wang, Z. H., Weng, G. Z., 1987. Late Carboniferous Conodonts from Southeastern Shanxi. In: The Coal Bearing Stratum of Late Paleozoic and its biota from southeastern Shanxi. Nanjing University Press, Nanjing. 281–291 (in Chinese)
- Wang, Z. H., Qi, Y. P., 2003. Review of Carboniferous-Permian Conodont Biostratigraphy in North China. *Acta Micropalaeontologica Sinica*, 20(3): 225–243 (in Chinese with English Abstract)
- Wang, Z. J., Gao, L. D., Zhang, Y. X., 1990. The Carboniferous System of China. Geological Publishing House, Beijing. 98–115 (in Chinese)
- Wardlaw, B. R., Boardman, D. R., Nestell, M. K., 2009. General Sequence Stratigraphy and Conodont Biostratigraphy (Including New Species) of the Uppermost Carboniferous (Upper Gzhelian) to Lower Permian (Lower Artinskian) from the North American Midcontinent. *Kansas Geological Survey Bulletin*, 255: 1–39
- Weng, W. H., Grabau, A. W., 1925. Carboniferous Formations of China. *X III Congress Geologogue International*, 2: 657–689
- Wu, B. J., Li, H. X., Joachimski, M. M., et al., 2021. Roadian-Wordian (Middle Permian) Conodont Biostratigraphy, Sedimentary Facies and Paleotemperature Evolution at the Shuixiakou Section, Xikou Area, Southeastern Qinling Region, China. *Journal of Earth Science*, 32(3): 534–553. <https://doi.org/10.1007/s12583-020-1099-y>
- Wu, Q., Ramezani, J., Zhang, H., et al., 2021. High-Precision U-Pb Age Constraints on the Permian Floral Turnovers, Paleoclimate Change, and Tectonics of the North China Block. *Geology*, 49(6): 677–681. <https://doi.org/10.1130/g48051.1>
- Xia, G. Y., Ding, Y. J., Zhao, S. Y., 1987. Subdivision of Carboniferous-Permian Fusulinid-Bearing Strata of Henan and Their Fauna. *Professional Papers of Stratigraphy and Palaeontology*, 17(1): 98–128 (in Chinese with English Abstract)
- Yang, C. H., Du, L. L., Song, H. X., et al., 2020. Geochronology and Petrogenesis of Neoproterozoic Yanzhuang Syenogranites from Sushui Complex in the Zhongtiao Mountains: Implications for the Crustal Evolution of the North China Craton. *Earth Science*, 45(9): 3161–3178. <https://doi.org/10.3799/dqkx.2020.254> (in Chinese with English Abstract)
- Yang, J. H., Cawood, P. A., Montañez, I. P., et al., 2020. Enhanced Continental Weathering and Large Igneous Province Induced Climate Warming at the Permo-Carboniferous Transition. *Earth and Planetary Science Letters*, 534: 116074. <https://doi.org/10.1016/j.epsl.2020.116074>
- Yang Z. L., Hu X. J., Wang S. Q., et al., 2021. Identification of Precambrian Strata in Early Paleozoic Accretion Zone on Southern Margin of Xing-Meng Orogenic Belt and Its geological Significance. *Earth Science*, 46(8): 2786–2803. <https://doi.org/10.3799/dqkx.2020.281> (in Chinese with English Abstract)
- Zakharov, Y. D., Bondarenko, L. G., Popov, A. M., et al., 2021. New Findings of Latest Early Olenekian (Early Triassic) Fossils in South Primorye, Russian Far East, and Their Stratigraphical Significance. *Journal of Earth Science*, 32(3): 554–572. <https://doi.org/10.1007/s12583-020-1390-y>
- Zhai, M. G., Santosh, M., 2013. Metallogeny of the North China Craton: Link with Secular Changes in the Evolving Earth. *Gondwana Research*, 24(1): 275–297. <https://doi.org/10.1016/j.gr.2013.02.007>
- Zhai, M. G., Santosh, M., 2011. The Early Precambrian Odyssey of the North China Craton: A Synoptic Overview. *Gondwana Research*, 20(1): 6–25. <https://doi.org/10.1016/j.gr.2011.02.005>
- Zhang, H. Q., 1989. Regional Geology of Henan Province. Geology Publishing House, Beijing. 185–189 (in Chinese)
- Zhang, N. M., 1990. Discovery of Upper Carboniferous Taiyuan Formation

- Conodonts in Xinggong-Xinmi Coal Fields, Western Henan. *Oil & Gas Geology*, 11(2): 209–213, 224 (in Chinese with English Abstract)
- Zhang, W. X., Quan, X. C., Wang, Y. J., et al., 2018. Study on Biostratigraphic Features of Deep Part Permo-Carboniferous Strata in Jiaxian Area, Northern Shaanxi. *Coal Geology of China*, 30(1): 16–21 (in Chinese with English Abstract)
- Zhang, W. S., Ding, H., Wan, S. L., 1988. The Conodont Sequence of the Taiyuan Formation and Boundary of Carboniferous-Permian in Dafengkou, Yuxian, County, Henan Province. *Shanxi Mining College Learned Journal*, 6(2): 104–113 (in Chinese with English Abstract)
- Zhang, X. J., Liang, X. Y., 1987. Ostracoda from the Taiyuan Formation of Xingyang and Gong Xian Districts, Henan. *Acta Micropalaeontologica Sinica*, 4(3): 293–312, 349 (in Chinese with English Abstract)
- Zhang, Z. C., Xia, G. Y., 1985. Fusulinid Zonation of the Upper Carboniferous Shanxi Formation, Southeastern Shanxi. *Regional Geology of China*, 4(2): 53–61, 127 (in Chinese with English Abstract)
- Zhao, G. C., Sun, M., Wilde, S. A., et al., 2005. Late Archean to Paleoproterozoic Evolution of the North China Craton: Key Issues Revisited. *Precambrian Research*, 136(2): 177–202. <https://doi.org/10.1016/j.precamres.2004.10.002>
- Zhao, J. M., Liang, X. Y., 1994. A Phaceloid Colonial Rugose Coral from Late Carboniferous Taiyuan Formation of Henan. *Acta Palaeontologica Sinica*, 33(5): 593–603, 663. <https://doi.org/10.19800/j.cnki.aps.1994.05.004> (in Chinese with English Abstract)
- Zhao, S. Y., 1981. Late Carboniferous Conodonts from the Qinshui Basin, Shanxi Province. *Geological Survey and Research*, 4: 97–108 (in Chinese with English Abstract)
- Zhao, S. Y., Wan, S. L., 1983. Some Conodonts from the Upper Carboniferous Kaiping Formation in Tangshan Area and Their Significance. *Geological Survey and Research*, 8: 95–104 (in Chinese with English Abstract)
- Zhao, S. Y., Wan, S. L., 1984. Subvolume of Micropaleontology. In: Atlas of Paleontology in North China. Geological Publishing House, Beijing. 253–254 (in Chinese)
- Zhao, S. Y., 1989. Carboniferous-Permian Conodonts in Longyin Area, Pu'an County, Guizhou Province, and Their Significance. *Bulletin Tianjing Institute Geology Mining Research*, 23: 141–159 (in Chinese with English Abstract)
- Zheng, H., 1987. Late Palaeozoic Small Foraminiferal Fauna from Yu Xian, Henan. *Acta Micropalaeontologica Sinica*, 4(2): 217–224, 256 (in Chinese with English Abstract)
- Zhong, R., Fu, Z. M., 1998. The Relationship between the Distribution of Thick Coal Belts and the Late Carboniferous-Early Permian Marine Transgression-Regression in the North China Platform. *Acta Geologica Sinica—English Edition*, 72(1): 114–120. <https://doi.org/10.1111/j.1755-6724.1998.tb00739.x>